The Astrophysical Journal, 595:279–284, 2003 September 20

CYCLOTRON MASER RADIATION FROM ASTROPHYSICAL SHOCKS

R. Bingham and B. J. Kellett
Rutherford Appleton Laboratory, Chilton, Didcot, Oxon OX11 0QX, UK

R. A. Cairns
University of St. Andrews, Fife, Scotland KY16 9SS, UK

J. Tonge
Department of Physics, University of California, Los Angeles, CA 90024

and

J. T. Mendonça
GoLP/Centro de Física de Plasmas, Instituto Superior Técnico, 1096 Lisboa Codex, Portugal
Received 2001 May 21; accepted 2003 April 28

ABSTRACT

One of the most popular coherent radio emission mechanisms is electron cyclotron maser instability. In this article we demonstrate that electron cyclotron maser emission is directly associated with particular types of charged particle acceleration such as turbulence and shocks commonly inferred in astrophysical plasmas.

Subject headings: masers — radiation mechanisms: nonthermal

1. INTRODUCTION

We present a model of coherent emission directly connected to the process of particle acceleration to high energies owing to collisionless shock waves, including the full relativistic effects. We consider acceleration by either plasma wave turbulence or quasi-perpendicular shocks. The particular plasma waves we consider propagate mainly perpendicular to the magnetic field, which can accelerate electrons by the surfatron process (Katsouleas & Dawson 1983). Both surfatron and shock acceleration provide us with velocity-space ring-type distribution functions, which we demonstrate are ideal for generating cyclotron maser radiation. A coherent emission mechanism would explain the high brightness measurements without having to rely on special geometrical effects. The model we propose is directly linked to the injection and acceleration of particles at shocks and does not need a second-stage process since it cannot be separated from the acceleration process. The radiation is a result of the relaxation process whenever an anisotropic distribution is formed.

The role of coherent emission mechanisms in explaining planetary solar and stellar observations is firmly established; for example, the emission from planetary magnetospheres is considered to be electron cyclotron maser radiation. It was first introduced by Twiss (1958) to explain radio astronomical sources. The electron cyclotron maser (Sprangle & Drobot 1977) is a collective electromagnetic emission producing intense extraordinary mode radiation close to the electron cyclotron frequency Ω_e, with small bandwidth.

The electron cyclotron maser instability is a powerful mechanism for producing nonthermal stimulated radiation in a plasma. The free energy source for the electron cyclotron instability giving rise to stimulated emission of radiation is an anisotropic electron distribution function such that $\partial f_e/\partial v_\perp > 0$, which constitutes a population inversion. The loss-cone distribution function with $\partial f_e/\partial v_\perp > 0$ is commonly considered as the free energy source (Wu & Lee 1979). However, in many situations where intense radio emission is observed, energetic particle beams are also observed or invoked. Electron beams propagating in a varying magnetic field give rise to a characteristically shaped horseshoe distribution as a result of the first adiabatic invariant. Horseshoe distributions also have $\partial f_e/\partial v_\perp > 0$, a necessary structure for generating radiation (Bingham & Cairns 2000). The horseshoe distribution is extremely efficient (Bingham & Cairns 2000) in generating cyclotron maser radiation; these previous treatments only considered weakly relativistic particles. The electron cyclotron maser produces stimulated emission with a narrow bandwidth polarized in the R-X mode and occurs in regions where the cold background plasma component is depleted in comparison to the hot component. The maser instability has maximum growth for low background plasma density, such that the beam density is greater than the ambient density. This is supported by satellite measurements of depleted density regions known as the auroral cavity, where a horseshoe electron distribution function is also observed (Ergun et al. 2000). Another type of electron distribution function invoked to explain nonthermal radiation from space and astrophysical objects is a ring-type distribution in perpendicular velocity space. The ring distribution is similar to those used in laboratory gyrotron devices where intense maser radiation is generated from relativistic electrons (Sprangle & Drobot 1977). In astrophysics, ring-type distributions can also be found, for example, at quasi-perpendicular shocks (Tokar et al. 1986).

The instability giving rise to electron cyclotron maser action in plasmas is driven by anisotropic velocity space distribution functions. Processes which are responsible for creating these anisotropic velocity space distributions are directly associated with particle acceleration mechanisms; therefore, any discussion of maser radiation mechanisms must consider acceleration processes. In particular, we consider acceleration processes which may occur in jets and give rise to particular anisotropic velocity space distributions suitable for driving the electron cyclotron maser emission. Plasma wave turbulence and shocks commonly inferred in astrophysics can provide the necessary free energy in the

form of anisotropic velocity space distributions to drive the maser emission mechanism.

1.1. *Electron Acceleration*

Models of electron acceleration in jets include acceleration by magnetohydrodynamic plasma wave turbulence or by shocks. Both processes are capable of producing highly relativistic particles with a power-law tail from a slightly relativistic seed population. However, for these processes to be effective in accelerating electrons, there must be waves that are in cyclotron resonance with the particles. In low-density plasmas likely to exist in jets, the electrons must be mildly relativistic before significant acceleration takes place by Alfvén wave resonance. This is the so-called injection problem, where electrons from a low-temperature thermal population are accelerated to subrelativistic velocities where Alfvén wave resonance is effective. Recent studies of electron acceleration by the surfatron acceleration mechanism (Katsouleas & Dawson 1983) demonstrate the effectiveness of this acceleration process in fulfilling the role of preinjector (McClements et al. 1993). There is no limit to the energy gained from this process. In practice, however, it is limited by the transverse dimensions of the plasma turbulence region or shock. The surfatron accelerator scheme was introduced by Katsouleas & Dawson (1983) to overcome the limit set by dephasing in relativistic plasma wave accelerators.

Surfatron acceleration is a wave particle acceleration scheme where waves such as Bernstein waves, lower hybrid, magnetosonic, and upper hybrid waves, which all propagate with a component of their electric field perpendicular to the ambient magnetic field, have a common damping mechanism resulting in energization of particles perpendicular to the magnetic field. These waves can easily be driven by ion beams propagating perpendicularly to the magnetic field. The energization mechanism can be of a stochastic or nonstochastic nature. Karney (1979) described stochastic heating of ions by lower hybrid waves as a random interaction of waves and particles with a resonant point in the particles' cyclotron orbit, where the particles receive kicks allowing them to increase in phase space. At a particular amplitude known as the stochastic threshold, significant heating is possible given by $\left(E/v_{\rm ph}B\right) = (1/4)(\omega/\Omega_e)^{1/3}$ (Karney 1979), where E is the wave field amplitude, ω is the wave frequency, $v_{\rm ph}$ is the phase velocity, and ω_{e0} is the cyclotron frequency ($= eB/m_e$). For wave amplitudes below this threshold amplitude we have the linear nonstochastic regime, for $(1/4)(\omega/\Omega_e)^{1/3} < E/v_{\rm ph}B < 1$ we are in the stochastic regime, and for $E/v_{\rm ph}B > 1$ we are in the nonstochastic nonlinear regime. Most attention has concerned the stochastic regime resulting in plasma heating. The nonstochastic regime has been concerned with particle acceleration for both nonrelativistic and relativistic particles. The essential elements of surfatron acceleration in the relativistic nonstochastic regime were derived by Katsouleas & Dawson (1983), although it had been used for both relativistic and nonrelativistic particle acceleration (Cairns 1971; Sagdeev & Shapiro 1973; Lembege & Dawson 1989; Lee, Shapiro, & Sagdeev 1996; Bingham et al. 2000). It was used to explain electron energization to overcome the main weakness of diffusive shock acceleration by providing an acceleration mechanism for low-energy particles known as the injection problem (McClements et al. 1997; Lee et al. 1996).

A test particle description of the surfatron acceleration model can easily be described using relativistic equations for the particle. Consider a magnetic field in the z-direction and a wave with a longitudinal electric field moving in the y-direction; then the equations of motion for an electron are

$$\frac{dp_x}{dt} = \frac{-eBp_y}{m_0\gamma}\,, \tag{1}$$

$$\frac{dp_y}{dt} = \frac{eBp_x}{m_0\gamma} - eE\sin(ky-\omega t)\,, \tag{2}$$

$$\frac{dy}{dt} = \frac{p_y}{\gamma m_0}\,, \tag{3}$$

where m_0 is the electron rest mass and p_i is the particles momentum ($= \gamma m_0 v_i$). If Ω_{e0} is the nonrelativistic cyclotron frequency (calculated with the rest mass $= eB/m_0$), we can normalize time in terms of $1/\Omega_{e0}$, length in units of c/Ω_{e0}, and momentum in units of $m_0 c$. We also transform the y coordinate such that $y \rightarrow y - (\omega/k)t$, where ω/k is the wave phase speed. Then we obtain the dimensionless equations of motion

$$\frac{dp_x}{dt} = -\frac{p_y}{\gamma}\,, \tag{4}$$

$$\frac{dp_y}{dt} = \frac{p_x}{\gamma} - \beta\sin(ky)\,, \tag{5}$$

$$\frac{dy}{dt} = \frac{p_y}{\gamma} - \alpha\,, \tag{6}$$

where $\alpha = \omega/k$ the wave phase speed, and $\beta = eE/mc\Omega_{e0}$.

Consider a solution to equations (4)–(6) in which there is steady acceleration of the particle. If $(dy/dt) = 0$, corresponding to no phase change of the particle with respect to the wave, then from equations (4) and (6) we get $(dp_x/dt) = -\alpha$. If we assume that at the same time $\left(dp_y/dt\right) = \eta$, and that we are in the asymptotic regime where

$$p_x \approx -\alpha t\,, \tag{7}$$

$$p_y \approx \eta t\,, \tag{8}$$

$$\gamma = \sqrt{1 + p_x^2 + p_y^2} \approx p_x^2 + p_y^2\,, \tag{9}$$

then equation (4) implies that

$$\alpha = \frac{-\eta}{\sqrt{\alpha^2+\eta^2}} \tag{10}$$

or

$$\eta = \alpha^2/\left(1-\alpha^2\right)^{1/2}\,. \tag{11}$$

We are assuming that $\alpha < 1$; i.e., the wave phase velocity is less than c. For these relations to be consistent with equation (5) we also need

$$\eta = -\frac{\alpha}{\sqrt{\alpha^2+\eta^2}} - \beta\sin(ky_0)\,, \tag{12}$$

where y_0 is the constant value of y. Rearranging equation (12) gives

$$-\beta\sin(ky_0) = \frac{1}{\sqrt{1-\alpha^2}}\,, \tag{13}$$

which has no possible solution unless

$$\beta \geq \frac{1}{\sqrt{1-\alpha^2}}\,. \tag{14}$$

Condition (14) gives a threshold wave amplitude above which we may expect to find solutions in which the particle travels along the wave front continuously gaining energy. The threshold value is $E \approx \gamma_{\rm ph} c\beta$, where $\gamma_{\rm ph} = [1/(1-\alpha^2)^{1/2}]$, which is the relativistic trapping threshold; a trapped particle satisfying $E = \gamma_{\rm ph} c\beta$ can never detrap.

The solutions of equations (4)–(6) are shown in Figure 1 for $\alpha = 0.3$, for which the critical β is 1.048. The initial run has $\beta = 1.05$, and we show a phase plane diagram for the momenta in Figure 1. Clearly the results approach an asymptotic solution of the form described above, with y tending to a constant value and the momentum and energy increasing linearly with time. The only constraint on the energy achieved is the spatial extent of the system. The results for many particles are close to being ring-type distributions in the perpendicular momentum space ideal for the generation of radiation by the cyclotron maser radiation mechanism. These ring distributions can be represented by the following distribution

$$f_{\rm ring}(p_\perp,\ p_\parallel) = \text{const.} \times \exp\left[-\frac{(p_\perp - p_0)^2}{m_e^2 v_{T_\perp}^2} - \frac{p_\parallel^2}{m_e^2 v_{T\parallel}^2}\right], \tag{15}$$

where p_0 is the ring momentum, $p_\parallel$ and $p\perp$ are the perpendicular and parallel momenta, $v_{T\perp}$ is the ring thermal speed, and $v_{T\parallel}$ is the parallel thermal speed. Such ring-type distributions have been observed in particle in cell simulations of collisionless shocks (Tokar et al. 1986) and magnetosonic waves (Lembege & Dawson 1989).

At quasi-perpendicular shocks, counterstreaming ion flows and ring distributions are also formed. These particular ion distributions are ideal for the generation of lower hybrid waves by the modified two-stream instability

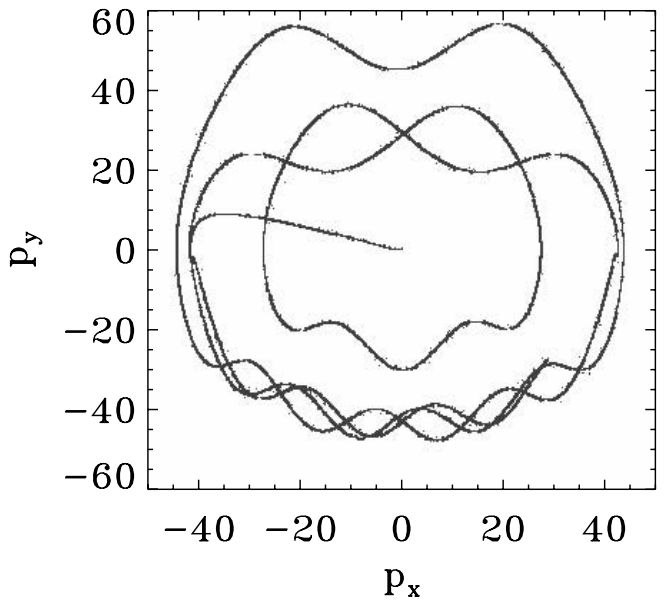

FIG. 1.—Numerical solutions of eqs. (4)–(6) for a wave phase speed $\alpha = \omega k = 0.3$, $k = 0.2$, and $\beta = 1.045$, depicting phase-plane diagram for the x and y components of the perpendicular momenta that form a ring perpendicular to the magnetic field.

(Bingham, Dawson, & Shapiro 2003). Lower hybrid waves are electrostatic waves that are in simultaneous Cerenkov resonance with ions propagating perpendicular to the magnetic field. The result is an energy transfer from ions to electrons or vice versa. In the modified two-stream instability ion beams or rings in velocity space generate lower hybrid waves that are capable of accelerating electrons parallel to the magnetic field to high energies. Numerical simulation studies (McClements et al. 1993) show that energetic electrons are easily produced, forming a high-energy tail or beam moving along the magnetic field lines. This beam will evolve into a horseshoe or crescent-shaped distribution function as it moves into a stronger field region as a result of the first adiabatic invariance, which states that $B/v_\perp^2$ is a constant. A magnetized collisionless shock is ideal for producing such distribution functions: the magnetic field increases going from upstream to the downstream region. The two types of electron distribution functions described above, namely, the ring and the horseshoe easily produce cyclotron maser radiation (Bingham & Cairns 2000), which we now demonstrate.

1.2. *Cyclotron Maser Radiation Mechanism*

First we examine the stability of a horseshoe type of electron distribution function for R-X mode waves propagating perpendicular to the steady magnetic field. To obtain the distribution function, we start with a drifting Maxwellian, with a drift velocity well above the thermal speed, which is typical of electrons accelerated by lower hybrid turbulence. This is then considered to move into an increasing magnetic field where the distribution function is readily calculated using invariance of total energy and magnetic moment. The distribution function is used in the dispersion relation for the R-X mode, which is easily obtainable from the susceptibility tensor given by Stix (1992).

We shall assume that the frequency is close to the electron cyclotron frequency and also assume that the Larmor radius is much less than the wavelength for typical electron velocities. This latter condition means that we need only consider the susceptibility to lowest order in $(k_\perp v_\perp)/\Omega_e$. If we neglect all but the zero-order terms, we get the cold plasma result. To a first approximation we need only take account of the velocity distribution of the electrons in the resonant integral which involves $1/(\omega - \Omega_e)$, where Ω_e is the relativistic electron cyclotron frequency $eB/\gamma m_e$, with e the electron charge, B the magnetic field, γ the Lorenz factor, and m_e the electron rest mass. In this resonant term we must take account of the relativistic shift of the cyclotron frequency, since this picks out a particular group of resonant electrons and produces damping or growth of the wave.

In terms of momentum p we have

$$\Omega_e = \Omega_{e0}\left(1 + \frac{p^2}{m^2 c^2}\right)^{-1/2},$$

where Ω_{e0} is the nonrelativistic electron cyclotron frequency. For the real part of the resonant integral we can simply take the cold plasma value. Although this goes as $1/(\omega - \Omega_{e0})$ and appears to be near singular at the resonance, the $1/(\omega - \Omega_{e0})$ factors in the real part of the dispersion relation cancel out, as we shall see, and it behaves quite smoothly in the vicinity of the cyclotron frequency. It is not crucial to include small corrections to the cyclotron

frequency in the real part of the dispersion relation. The refractive index n for the R-X mode, which propagates perpendicular to the magnetic field, is given by (Stix 1992)

$$n^2 = \left(\epsilon_\perp^2 - \epsilon_{xy}^2\right)/\epsilon_\perp \,, \tag{16}$$

and the dielectric tensor elements are given by

$$\epsilon_\perp = 1 - \frac{1}{2}\frac{\omega_p^2}{\omega(\omega + \Omega_{e0})} + A \,, \tag{17}$$

$$\epsilon_{xy} = \frac{1}{2}\frac{\omega_p^2}{\omega(\omega + \Omega_{e0})} + A \,, \tag{18}$$

with

$$A = \frac{1}{4}\frac{\omega_p^2}{\omega}\int_0^\infty 2\pi p_\perp dp_\perp \int_{-\infty}^\infty dp_\parallel \frac{1}{\omega - \Omega_e} p_\perp \frac{\partial f_0}{\partial p_\perp} \,. \tag{19}$$

To obtain this we have included only the ± 1 terms in the sum over harmonics, which appears in the dielectric tensor elements, and used the small argument expansion $J_1(x) \approx (x/2)$, where $x = (k_\perp v_\perp)/\Omega_e$ changing the variables to $(p,\ \mu,\ \phi)$, spherical polars with the usual angle θ replaced with $\mu = \cos\theta = p_\parallel/p$; then

$$A = -\frac{1}{2}\frac{\omega_p^2}{\omega(\omega - \Omega_0)} - \frac{i}{2}\frac{\omega_p^2}{\Omega_0}\int_1^{-1} (1-\mu^2) p_0^2 \gamma_0^2 \times \left\{\frac{\partial f_0}{\partial p} - \frac{\mu}{p_0}\frac{\partial f_0}{\partial \mu}\right\} | p = p_0 | d\mu \,, \tag{20}$$

where $\gamma = (1 + p^2)^{1/2}$ and p_0 is the resonant momentum given by $mc[2(\Omega_{e0} - \omega)\Omega_e]^{1/2}$. A full discussion of the derivation of the dispersion relation for perpendicularly propagating waves can be found in Stix (1992).

Using equation (19) in equations (17) and (18) we can analyze the stability of equation (16) with respect to induced emission of right hand polarized radiation.

The initial beam is considered to be a drifting Maxwellian. Figure 2 illustrates the characteristic crescent or horseshoe distribution formed when the beam moves into a stronger field region. Using the evolved distribution in equation (16), we obtain the spatial growth rate shown in Figure 3 for two initial beam energies. Figures 3*a* and 3*b* represent the imaginary part of the refractive index as a function of frequency for a mean beam energy of 100 keV (Fig. 3*a*) and 500 keV (Fig. 3*b*), both with a 1% energy spread and a magnetic field ratio of 20. The maximum growth rate for the 500 keV beam is more than 4 times greater than for the 100 keV beam. The analysis presented above considers strictly perpendicular propagation. However, we have calculated the growth rates for modes that also contain a parallel wavenumber component and find that modes that propagate more than about 5^0 to the perpendicular do not grow. The fastest growing component is for purely perpendicular propagation. The region of instability in frequency space is extremely narrow with a bandwidth $\Delta\omega/\omega$ on the order of 0.5%.

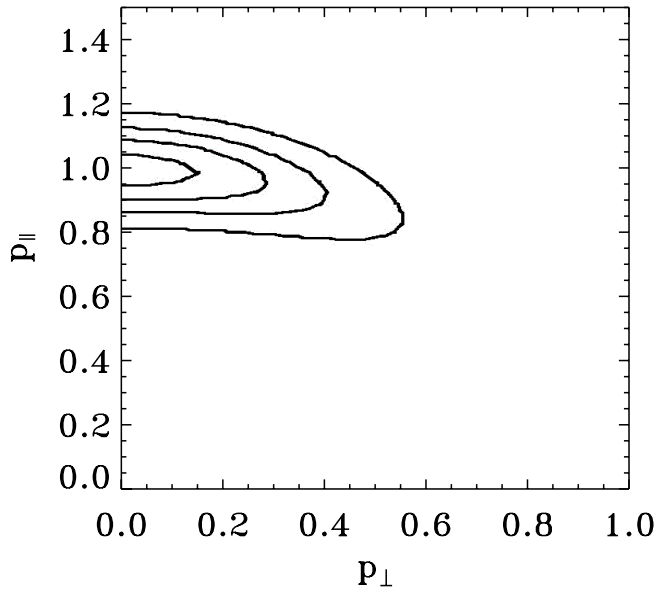

FIG. 2.—Contour plot in momentum space of the perpendicular and parallel electron momentum components of the evolved horseshoe distribution function. The contours represent constant phase-space density.

We now consider the case of a velocity ring distribution shown in Figure 4. The ratio of the ring density to background density is 0.2 and a ring energy much greater than the Maxwellian background. Again using the distribution function defined by equation (15), in equation (16) we obtain the spatial growth rate for a ring distribution shown in Figure 5. It should be noted that the emission from a horseshoe or ring distribution is primarily in the plane perpendicular to the magnetic field, and the emission is close to the cyclotron frequency. For higher energy beams or rings the frequency decreases because of the relativistic mass increase.

A parallel component of wavenumber introduces a Doppler shift into the resonance condition, so that the resonant particles no longer lie on a sphere centered on the origin in momentum space. This means, in turn, that for any significant Doppler shift, the resonant particles will no longer all lie in the part of the distribution function where there is a positive slope toward increasing energy. For this reason the growth rate will fall off as we go away from perpendicular propagation, and the maximum emission is expected to be in the perpendicular direction. The instability is found to be sensitive to the ratio of the cyclotron frequency to the plasma frequency Ω_{ce}/ω_{pe}. The instability would be expected to occur in regions of low-background plasma density, where two-stream and other instabilities are not strong enough to disrupt the beam. Two-stream instabilities have growth rates that are proportional to ω_{pe} (Krall & Trivelpiece 1973), whereas the instability described here is not strongly dependent on density.

2. SUMMARY AND CONCLUSIONS

In this article we have developed an analytical approach describing the cyclotron maser instability convective spatial growth rate. Various types of distribution functions similar to those found at shocks lead to rapid growth of R-X mode radiation. We suggest that the spreading in perpendicular velocity as a beam moves into a region of increasing magnetic field or the formation of a velocity ring distribution, both produced at collisionless shocks, may trigger the instability and radio emission. Our model seems to be capable of explaining, at least in outline, the strong radio emission from shock waves, the importance of low-density regions, and the fact that the emission is perpendicular to the magnetic field. However, it is clear that a lot more detailed work

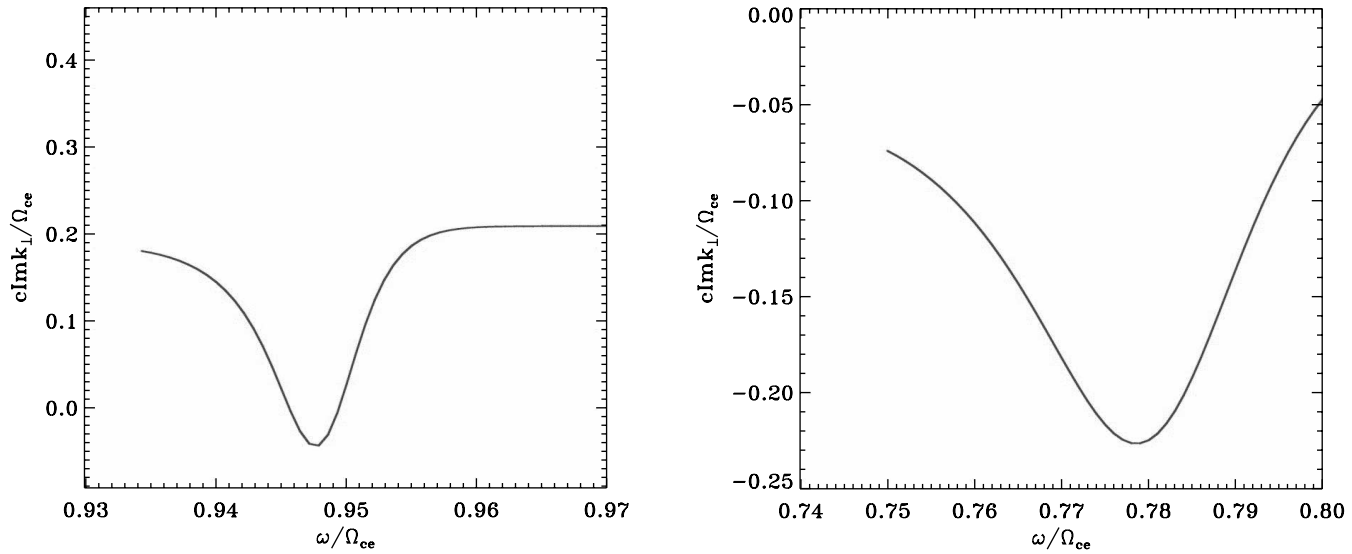

FIG. 3.—(*a*) Imaginary part of the refractive index as a function of frequency for a mean beam energy of 100 keV and a thermal spread of 1 keV. The magnetic field ratio is taken to be 20. (*b*) Same as (*a*), except the mean beam energy is 500 keV and the spread is 5 keV.

is needed to bring the various aspects together into a comprehensive model. Future particle in cell simulations will investigate self-consistently the instability starting with an isotropic beam moving into a stronger magnetic field, which will reveal a more realistic comparison with the observations. The model presented is also consistent with acceleration processes associated closely with shock waves. We have not considered the Doppler boost; this is possible if the shocks are relativistic and will be a mechanism to spread the wave frequency. Variations of magnetic field strength at the shock will also act to spread the wave frequency.

We would like to pay tribute to the late Professor John Dawson, who played such an important role in this research.

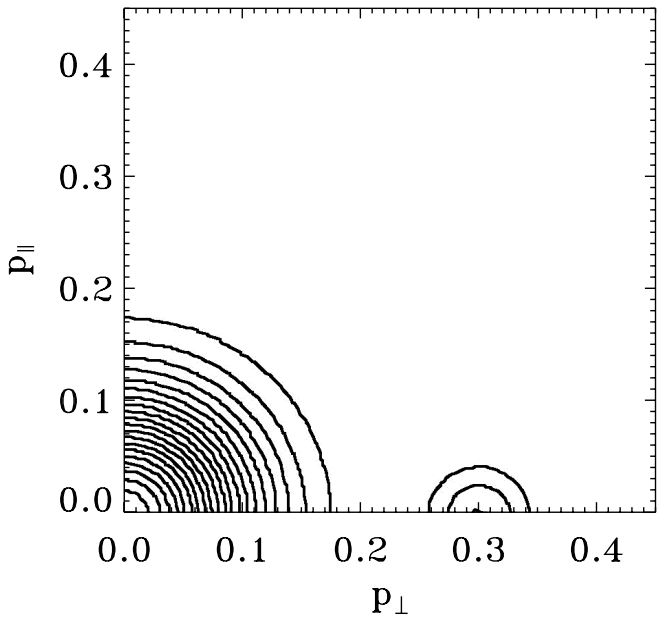

FIG. 4.—Contour plot in momentum space of the electron momentum components depicting a background Maxwellian and a perpendicular ring distribution. The ratio of ring electron density to background Maxwellian density is 0.2.

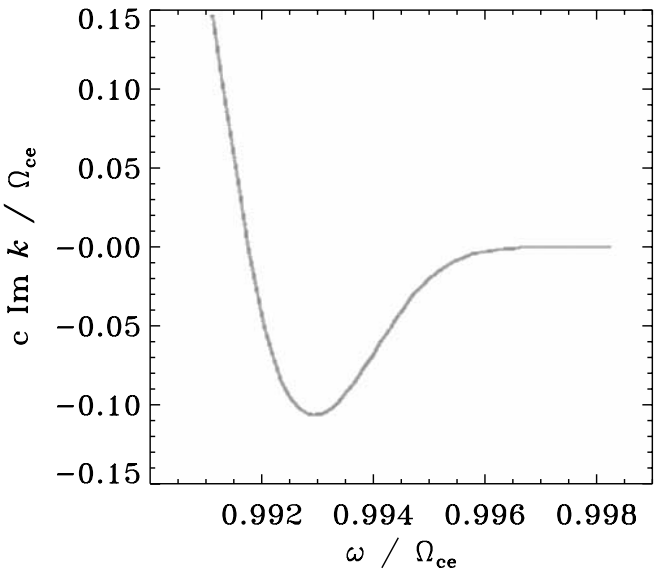

FIG. 5.—Spatial growth rate $Imk_\perp$ of the R-X mode for the ring distribution shown in Fig. 4.

REFERENCES

Bingham, R., & Cairns, R. A. 2000, Phys. of Plasmas 7, 3089
Bingham, R., Cairns, R. A., & Menconça, J. T. 2000, J. Plasma Phys., 64, 481
Bingham, R., Dawson, J. M., & Shapiro, V. D. 2003, J. Plasma Phys., 68, 161
Cairns, R. A. 1971, J. Plasma Phys., 13, 725
Ergun, R. E., Carlion, C. W., McFadden, J. P., Delory, G. T., Strangway, R. J., & Pritchett, P. L. 2000, ApJ, 538, 456
Karney, C. F. F. 1979, Phys. Fluids B, 21, 1584
Katsouleas, T., & Dawson, J. M. 1983, Phys. Rev. Lett., 51, 392
Krall, N., & Trivelpiece, A. W. 1973, Principles of Plasma Physics (New York: McGraw Hill)
Lee, M., Shapiro, V. D., & Sagdeev, R. Z. 1996, J. Plasma Phys., 101, 4777
Lembege, B., & Dawson, J. M. 1989, Phys. Fluids B, 1, 1001
McClements, K. G., Bingham, R., Su, J. J., Dawson, J. M., & Spicer, D. S. 1993, ApJ, 409, 465
McClements, K. G., Dendy, R. O., Bingham, R., Kirk, J. G., & Drury, L. O'C. 1997, MNRAS, 291, 241
Sagdeev, R. Z., & Shapiro, V. D. 1973, J. Exp. Theor. Phys., 17, 279
Sprangle, P., & Drobot, A. T. 1977, Proc. IEEE, 25, 528
Stix, S. H. 1992, Waves in Plasmas (New York: AIP)
Tokar, R. L., Aldrich, C. H., Forslund, D. W., & Quast, K. B. 1986, Phys. Rev. Lett., 56, 1059
Twiss, R. Q. 1958, Australian J. Phys., 11, 564
Wu, C. S., & Lee, L. C. 1979, ApJ, 230, 621